



Universidade do Minho
Escola de Medicina

Ana Rita Lima Pinheiro

Development of genetically encoded biosensors for *Plasmodium falciparum*



Universidade do Minho
Escola de Medicina

Ana Rita Lima Pinheiro

Development of genetically encoded biosensors for *Plasmodium falciparum*

Dissertação de Mestrado
Mestrado em Ciências da Saúde

Trabalho efetuado sob a orientação de
Doutor Pedro Eduardo Ferreira

dezembro 2021

Direitos de autor e condições de utilização do trabalho por terceiros

Este é um trabalho académico que pode ser utilizado por terceiros desde que respeitadas as regras e boas práticas internacionalmente aceites, no que concerne aos direitos de autor e direitos conexos. Assim, o presente trabalho pode ser utilizado nos termos previstos na licença abaixo indicada. Caso o utilizador necessite de permissão para poder fazer um uso do trabalho em condições não previstas no licenciamento indicado, deverá contactar o autor, através do RepositóriUM da Universidade do Minho.

Licença concedida aos utilizadores deste trabalho



Atribuição

CC BY

<https://creativecommons.org/licenses/by/4.0/>

Agradecimentos

No final desta etapa, só posso agradecer a todos os que estiveram ao meu lado e a tornaram possível. Foi uma jornada de enriquecimento pessoal e científico.

Em primeiro lugar, gostaria de agradecer ao meu orientador, Pedro Ferreira, pelo apoio, motivação, conhecimento científico e por acreditar em mim desde o primeiro dia.

Aos membros do meu grupo, um agradecimento especial por toda a ajuda e paciência, por toda a partilha e preocupação. À Adriana, em especial, agradeço o simples facto de ter escolhido a nossa equipa, partilhar este caminho contigo foi incrível. Obrigada pela tua calma, por seres o meu equilíbrio e pela tua amizade.

Aos meus colegas de laboratório, quero agradecer por toda a partilha de conhecimento e pelo cuidado comigo. Em particular, aos malariosos que foram essenciais nas minhas dúvidas e inseguranças. Um agradecimento especial às minhas - MJ, Frias, Anita e Consuelo - por todo o brainstorm, os cafés, as conversas sem fim.... Tenho muita sorte de vos ter, fizeram este percurso mais leve e divertido.

A todos os meus amigos pelo apoio e suporte, por estarem sempre presentes, mesmo nos momentos de mau humor e nas crises existenciais. Um agradecimento especial às Sweeties e Cusquice, as vossas parvoíces e apoio tornaram os meus dias melhores.

Ao André que teve uma paciência ilimitada para minhas dúvidas existenciais e que nunca me deixou baixar os braços. Obrigada por veres sempre o lado bom, pela confiança, pelos abraços e por estares sempre ao meu lado, não podia pedir melhor.

Por fim, quero agradecer à minha família. Obrigada por todo o incentivo e apoio. O vosso cuidado, mimo e motivação foram a minha bomba de oxigénio. Um grande agradecimento à minha mãe, a tua força e amor inspiram-me a ser melhor a cada dia. A ti devo a minha jornada até aqui e sou eternamente grata por te ter.

The work presented in this thesis was performed in the Life and Health Sciences Research Institute (ICVS), University of Minho. Financial support was provided by grants from the National funds, through the Foundation for Science and Technology (FCT) - project UIDB/50026/2020 and UIDP/50026/2020, IF/00143/2015/CP1294/CT0001 and PTDC/SAU-PAR/28066/2017.



Statement of integrity

I hereby declare having conducted this academic work with integrity. I confirm that I have not used plagiarism or any form of undue use of information or falsification of results along the process leading to its elaboration.

I further declare that I have fully acknowledged the Code of Ethical Conduct of the University of Minho.

Resumo

A malária é uma das principais doenças em todo o mundo, com mais de 200 milhões de infecções e aproximadamente 500 mil mortes associadas. A maior incidência ocorre em crianças até dos 5 anos. O *P. falciparum* é o *Plasmodium spp* mais virulento, causando a maioria das mortes e os casos mais graves da doença.

Os medicamentos antimaláricos são usados mundialmente como a primeira linha de defesa. Dentro desta categoria, as terapias combinadas de artemisinina (ACTs) apresentam a maior eficácia no controle dos sintomas e na redução da taxa de infecções. No entanto, resistência do parasita aos antimaláricos é um problema transversal aos tratamentos disponíveis. Assim, urge compreender melhor os mecanismos moleculares subjacentes à resistência aos medicamentos contra a malária.

O metabolismo redox é um sistema ubíquo associado à maioria dos processos celulares. Este é crucial para o desenvolvimento do parasita, defesa antioxidante e está envolvido em mecanismos de ação e resistência a fármacos. Este, para além de essencial para a sobrevivência do parasita no ciclo assexuado, está também associado à resistência à CQ e, mais recentemente, à resistência a ACTs.

Contudo, a falta de ferramentas moleculares para estudar este organismo limita o conhecimento da sua biologia, das interações parasita-hospedeiro e dos mecanismos de ação das drogas. O sensor hGrx1-roGFP2 é um biossensor fluorescente geneticamente codificado, testado com sucesso em estudos redox em *P. falciparum*. Tem sido descrito como uma ferramenta poderosa na compreensão do metabolismo redox do parasita, possibilitando estudos *in vitro* em tempo real.

Tendo estas informações como base, nesta dissertação propomos o desenvolvimento de novos sensores para aprofundar o estudo dos mecanismos básicos em *P. falciparum*. O nosso objetivo é exportar hGrx1-roGFP2 para o eritrócito parasitado e realizar estudos de interação parasita-hospedeiro. Para isso, o sinal peptídico PEXEL - um motivo de transporte, que sinaliza proteínas para exportação - será acoplado ao sensor e integrado no genoma do parasita. O desenvolvimento de um biossensor com emissão no comprimento de onda do vermelho é também um objetivo. Se realizados com sucesso, esses sensores possibilitarão diferentes análises do comportamento redox do parasita.

Palavras chave: *Plasmodium falciparum*; metabolismo; redox; biossensores

Abstract

Malaria is one of the major illnesses worldwide. The highest incidence occurs in children under five years. *P. falciparum* is the most virulent *Plasmodium spp.* causing the majority of the deaths and the most severe cases of the disease.

Antimalarial drugs are used worldwide as a first-line defense against the disease, with the artemisinin combined therapies (ACTs) being the most effective in controlling the disease symptoms and slowing the rate of infections. However, an antimalarial resistance problem is widespread for most treatments deployed against *P. falciparum*. Therefore, urges to better understand the molecular mechanisms underlying drug resistance.

Intracellular redox metabolism is a ubiquitous system associated with most cellular processes. This metabolism is crucial for redox balance and antioxidant defense and is involved in drug action and resistance mechanisms. Besides the fact that it is vital for erythrocytic stage survival, glutathione is also engaged in CQ resistance and, more recently, has been associated with ACTs resistance.

It is crucial to better understand the biology of the parasite. However, the lack of molecular tools for this organism limits the knowledge of parasite-host interactions and mechanisms of drug action. hGrx1-roGFP2 is a fluorescent genetically encoded biosensor successfully tested in *P. falciparum* redox studies. It has been described as a powerful tool in understanding the parasite redox metabolism, as it makes possible *in vitro* real-time studies.

Therefore, we propose to develop new genetically encoded biosensors to go deeper in the study of fundamental mechanisms in *P. falciparum*. We aim to export hGrx1-roGFP2 into the parasitized erythrocyte and perform parasite-host interaction studies. For this, the signal peptide PEXEL - a trafficking motif that signals proteins to export - will be coupled to the sensor and integrated into the *P. falciparum* genome. We also propose to develop a biosensor with red fluorescence emission. If successfully made, these sensors will be able to perform different analyses of the parasite redox behavior.

Keywords: *Plasmodium falciparum*; metabolism; redox; biosensor

Table of Contents

Direitos de autor e condições de utilização do trabalho por terceiros	ii
Agradecimentos	iii
Statement of integrity	iv
Resumo.....	v
Abstract	vi
Table of Contents	vii
Table Index	x
List of Abbreviations and Acronyms.....	xi
1. Introduction	1
1.1 Malaria Epidemiology.....	1
1.2 Malaria infection	2
1.3 <i>Plasmodium falciparum</i>	2
1.3.1 Life cycle	3
1.4 Malaria control.....	4
1.5 Antimalarial Drugs.....	5
1.5.1 Quinolines.....	5
1.5.2 Antifolate Drugs.....	6
1.5.3 Artemisinin-based combination therapy.....	6
1.6 Antimalarial drug resistance	7
1.7 Redox Metabolism	7
1.8 Genetically encoded biosensors.....	8
1.8.1 hGrx1-roGFP2	8
1.8.2 hGrx1-roGFP2-PEXEL	10
1.8.3 hGrx1-roGFP2-PEXEL-DD	10
1.8.4 hGrx1-roRFP	11
1.9 Genetic engineering – Bxb1 integrase system	11

2. Aims.....	13
3. Materials and Methods.....	14
3.1 Plasmids construction	14
3.1.1 pJET_PEXEL construction.....	14
3.1.2 pDC2_hGrx1_roGFP_PEXEL construction.....	15
3.1.3 pDC2_hGrx1_roGFP_PEXEL_DD construction.....	16
3.1.4 pDC2_roRFP construction	16
3.1.5 Plasmids preparation for transfection	17
3.2 <i>P. falciparum</i> transgene cell lines.....	17
3.2.1 <i>P.falciparum</i> culture	17
3.2.2 <i>P. falciparum</i> growth analysis	18
3.2.3 <i>P. falciparum</i> transfection	18
3.2.4 Selection of parasites	19
3.2.5 Genotyping	19
3.3 Phenotyping	20
3.3.2 Shield assay on 3D7_PEXEL_DD	20
3.3.3 Confocal microscopy of Hb3_roRFP	21
3.3.4 Test of genetically encoded redox biosensor activity	21
3.3.5 Statistical Analysis	21
4. Results and Discussion	22
4.1 PEXEL and PEXEL_DD.....	22
4.1.1 Plasmids pDC2_hGrx1_roGFP_PEXEL and pDC2_hGrx1_roGFP_PEXEL_DD	22
4.2 roRFP genetically encoded biosensor	25
4.2.1 pDC2_roRFP.....	26
5. Conclusion	31
Bibliography.....	32

Figure Index

Figure 1. Countries with indigenous malaria cases in 2000 and their status in 2019.	1
Figure 2. <i>Plasmodium falciparum</i> life cycle..	4
Figure 3. Redox balance in <i>P. falciparum</i>	8
Figure 4. Schematic representation of the hGrx1-roGFP2 mode of action..	9
Figure 5. <i>Plasmodium spp.</i> genetic manipulation using the Bxb1 integrase system.....	12
Figure 6. Strategy and plasmid construction for pDC2_hGrx1_roGFP_PEXEL and pDC2_hGrx1_roGFP_PEXEL_DD.....	23
Figure 7. Genotyping and fluorescence excitation of parasites from 3D7 ^{attB} roGFP_PEXEL_DD.	24
Figure 8. Genotyping of plasmids pJET_roRFP and pDC2_gGrx1_roRFP.....	26
Figure 9. Confocal microscopy of Hb3 roGFP and roRFP lines.	27
Figure 10. Validation of efficacy of the genetically encoded fluorescent biosensor in response to redox stimulus.....	28
Figure 11. Comparison of Hb3 roRFP and Hb3 roGFP biosensors response to different oxidative statuses.	29

Table Index

Table 1. Primer sequences for plasmid construction.	16
Table 2. Primers sequence and PCR program for 3D7_PEXEL and 3D7_PEXEL_DD genotyping.	20

List of Abbreviations and Acronyms

ACTs	Artemisinin-based Combination Therapies
AQ	Amodiaquine
ART	Artemisinin
bp	Base pairs
BSD	Blasticidin
CQ	Chloroquine
DD	Destabilization domain
DDT	Dichloro-diphenyl-trichloroethane
DTT	Dithiothreitol
DV	Digestive vacuole
EMA	European Medicines Agency
ER	Endoplasmatic reticulum
G418	Neomycin
gDNA	Genomic DNA
GFP	Green fluorescent protein
GR	Glutathione reductase
GSH	Glutathione
GSSH	Glutathione disulfide
GST1	Glutathione S-transferase 1
GTS	Global technical strategy
HF	Halofantrine
hGrx1	human glutaredoxin-1
IVCC	Innovative Vector Control Consortium
LB	Lysogeny broth
LLIN	Long-lasting insecticide nets
LUM	Lumefantrine
MCM	Malaria culture medium
MQ	Mefloquine

P	Primer
PBS	Phosphate buffered saline
PCR	Polymerase chain reaction
PMQ	Primaquine
PMV	Plasmepsin V
PQ	Piperaquine
PTEX	<i>Plasmodium</i> translocon of exported proteins
QN	Quinine
RBC	Red blood cell
RFP	Red fluorescent protein
roGFP	Redox sensitive green fluorescent protein
roRFP	Redox sensitive red fluorescent protein
ROS	Reactive oxygen species
rpm	Rotations per minute
SEM	Standard error of the mean
SOC	Super optimal broth with catabolite repression
WHO	World Health Organization
WT	Wild type

1. Introduction

1.1 Malaria Epidemiology

Malaria remains one of the major concerns in public health. In 2019 an estimated 229 million cases were leading to 409 thousand deaths. Most of the recorded deaths are in children under five years, representing 67% of the total deaths. There are still 87 endemic malaria countries. The most threatened region is Africa, gathering 82% of the cases and 94% of the deaths (World Health Organization, 2020).

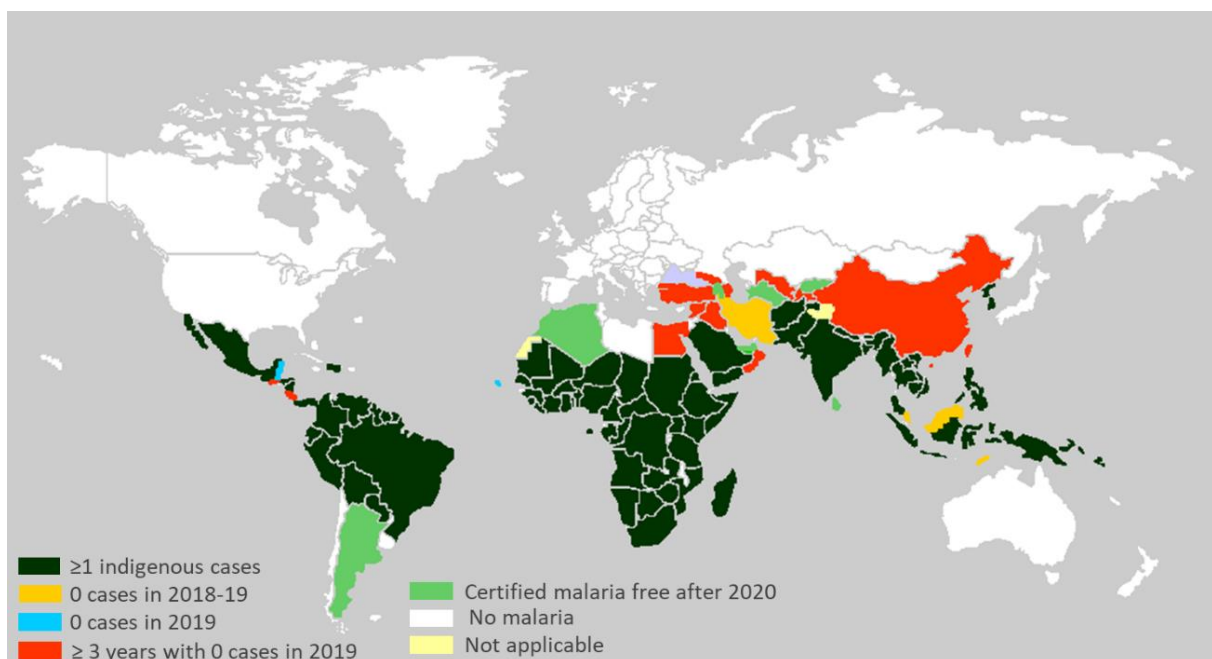


Figure 1. Countries with indigenous malaria cases in 2000 and their status in 2019. Distribution of malaria cases in 2019 in declared indigenous malaria countries in 2000. Based on World Malaria Report 2020 (World Health Organization, 2020).

Despite this, there have been successful efforts in malaria control, and since 2000 malaria rates have been decreasing. The number of countries with endemic malaria that reported fewer than 10 000 cases increased from 26 in 2000 to 46 in 2019. The malaria incidence is also reducing from 80 cases per 1000 in 2000 to 57 in 2019 (World Health Organization, 2020). These numbers are mostly related to control and elimination programs (Cotter et al., 2013). Another major factor is the use of artemisinin (ART) – based combination therapies (ACTs), along with insecticide-treated mosquito nets, improved healthcare systems, increased urbanization, and reduced poverty (Weiss et al., 2019). However, since 2015 reports have

shown a slowing of the rate of decline. From 2000 to 2015, the incidence of malaria infections decreased 27%, and between 2015 and 2019, it has only declined 2% (World Health Organization, 2020). The mortality caused by malaria has been reducing continuously since 2000, with 736 000 deaths in 2000 and 409 000 in 2019. Even the children's death incidence decreased, representing 84% of the total deaths in 2000 and 67% in 2019. In the latest years, the decline in mortality rate is also slower, reducing from 25 to 12 between 2000-2015 and 10 in 2019 (World Health Organization, 2020). The observed slowdown in the impact of malaria control measures indicates that novel and better interventions are needed to reduce malaria prevalence worldwide.

1.2 Malaria infection

Malaria is caused by a parasitic infection with the genus *Plasmodium* protozoan. It is a vector-borne disease that is transmitted through the bites of infected female *Anopheles spp.* mosquitoes (White et al., 2014). A wide variety of organisms can be infected with different species of *Plasmodium*. Only six species are known to cause disease in humans from this variety: *P. falciparum*, *P. vivax*, *P. malariae*, *P. ovale curtisi*, *P. ovale wallikeri*, and *P. knowlesi* (Pannu, 2019). *P. ovale* and *P. vivax* can assume a latent form, hypnozoite, that can reactivate the infection months or years later (Ross & Fidock, 2019). *P. falciparum* and *P. vivax* cause most of the cases worldwide. *P. vivax* has a more extensive distribution globally due to its ability to survive in a broader range of conditions (World Health Organization, 2020).

Different clinical outcomes can result from malaria infection. These can go from acute fever to organ failure, affecting lungs, liver, kidney, and the brain in cases of cerebral malaria, leading to respiratory distress, metabolic acidosis, coma, or death (Pannu, 2019; Ross & Fidock, 2019).

1.3 *Plasmodium falciparum*

P. falciparum is the *Plasmodium spp.* responsible for the most severe clinical manifestations of disease, mainly due to its ability of cytoadherence (Plewes et al., 2019). This species is most prevalent in Africa and causes most deaths associated with malaria, and is also the main species associated with drug resistance (World Health Organization, 2020).

1.3.1 Life cycle

P. falciparum has a complex life cycle alternating between two hosts: the Anopheles mosquito, where the sexual stage of development occurs, and the human host, characterized mainly by a pronounced asexual multiplication (Figure 2) (Josling & Llinás, 2015). On the human host, the infection starts when an infected Anopheles female mosquito takes a blood meal while injecting sporozoites into the bloodstream. Sporozoites migrate through the bloodstream to the liver, readily invading hepatocytes. In the liver stage, which takes approximately one to two weeks, the sporozoites undergo an asexual maturation process into multinucleated cells, the schizonts, that produce thousands of mononucleated merozoites. The hepatocytes eventually rupture, and the merozoites are released into the bloodstream. In the bloodstream, the merozoites invade the erythrocytes and start an intraerythrocytic 48-hour replication cycle. The merozoites, in the erythrocytes, develop into different morphological forms passing from ring forms (early trophozoites), late trophozoites, and schizonts containing multiple merozoites. Infected erythrocytes ultimately lyse, releasing the merozoites ready to infect new erythrocytes. This cyclic and synchronized rupture of the erythrocytes causes the febrile clinical manifestations of malaria. A minority of the merozoites do not undergo the intraerythrocytic replication cycle but instead differentiate into gametocytes. Circulating gametocytes in the human host bloodstream, which do not cause symptoms, can be taken by a mosquito during a blood meal. The microgametes (male) and macrogametes (female) fuse in the mosquito midgut to form the zygote. The zygote further develops into an ookinete that penetrates the gut wall, where the ookinete differentiates into an oocyst. Through meiosis, the oocyst becomes haploid and, through mitotic division, produces multiple sporozoites. After maturation, the oocyst ruptures, releasing the sporozoites, which migrate to the mosquito salivary glands, ready to infect a new human host and re-starting the parasite life cycle (Krishnan & Williamson, 2018; Sato, 2021; Zekar & Sharman, 2020).

Despite all the efforts made, the rate of decline in malaria cases and deaths is slowing down (World Health Organization, 2020). The investment of money and research in the discovery of vaccines has been hugely made. However, only in 2016, a vaccine received a positive recommendation from the European Medicines Agency (EMA) for an introduction test in Malawi, Ghana, and Kenya. So the impact of vaccines on malaria control is yet to be evaluated in the following years (World Health Organization, 2020).

1.5 Antimalarial Drugs

Antimalarial drugs are the most important tool in controlling and treating malaria. The use of chemotherapy remounts to the 17th century with plant-based products from cinchona to control fevers evolving up to nowadays with artemisinin combinations therapies (Cowman et al., 2016a).

1.5.1 Quinolines

In the 19th century, a significant advance was achieved with the isolation of the main active compound of these cinchona extracts, quinine (QN) (Sato, 2021). Although the rapid loss of effect due to emerging of resistance, QN was crucial for the development of several compounds that form the quinoline family – chloroquine (CQ), amodiaquine (AQ), piperazine (PQ), primaquine (PMQ), mefloquine (MQ), halofantrine (HF) and lumefantrine (LUM). The mechanisms and pathways involved in the action of these drugs remain unknown. The CQ mechanism of action is the most well-known from this group, and studies indicate that it is involved with parasite detoxification systems. During the intraerythrocytic cycle, mainly in the trophozoite stage, *P. falciparum* takes large amounts of hemoglobin into the digestive vacuole (DV) as a source of amino acids (Wellems & Plowe, n.d.). Hemoglobin digestion leads to the release of the reactive heme and reactive oxygen species (ROS), which are toxic for the parasite. The clearance of these compounds is in charge of detoxification systems. By targeting these processes, CQ leads to parasite loss of function and death through toxification (Combrinck et al., 2013).

1.5.2 Antifolate Drugs

Another important class of drugs in the fight against malaria is folates. The folate biosynthesis pathway is involved in several cellular mechanisms such as DNA synthesis, particularly in the last stages of the intraerythrocytic phase, being crucial for parasite survival. The two main drugs of this family are sulfadoxine and pyrimethamine, often used combined. These drugs bind and inhibit two enzymes of the folate biosynthesis pathway, which disrupt the flow of the parasite lifecycle (Sridaran et al., 2010).

1.5.3 Artemisinin-based combination therapy

Artemisinin derivatives (ARTs) and artemisinin combination-based therapies (ACTs) are the recommended chemotherapy for the first-line treatment of malaria by WHO (Kano, 2010). These drugs act rapidly on the intraerythrocytic stage of malaria. They need to be activated, and this activation happens when hemoglobin degradation, made by the parasite, liberates free heme, which promotes the cleavage of the endoperoxide bridge of the drug. The consumption of hemoglobin is essential for parasite growth (Blasco et al., 2017; Talman et al., 2019). ART promotes rapid clearance rates of parasite loads in a single intraerythrocytic cycle (48h). For total recovery from malaria infection, a 7-day treatment plan is needed when using artemisinin as monotherapy (Ferreira et al., 2013). However, this drug has a short *in vivo* half-life problem, approximately 1 hour (Talman et al., 2019). Due to that, ARTs administration is combined with a long-lasting partner drug with a distinct proposed mechanism of action. The combinations prevent exacerbation and re-emergence of the infection. Besides, they diminish the risk and pace of resistance development, which is the main problem in malaria treatment (Eastman & Fidock, 2009; White, 2013). Some studies suggest that ARTs' efficacy against the parasites in their activated state results from their reaction with susceptible groups in biomolecules, including heme, proteins, and lipids, leading to oxidative stress and cellular damage (Mishra et al., 2017; Talman et al., 2019).

1.6 Antimalarial drug resistance

As mentioned previously, chemotherapy treatments have been an essential tool in the fight against malaria. However, *P. falciparum* resistance is transversal to almost all the available drugs, even for the ACTs. This resistance was firstly reported in South Asia, mainly in Cambodia, but it is spreading worldwide (Dondorp et al., 2009). There are also reported cases in South America (Douine et al., 2018) and it was already detected in the Sub-Saharan Region, which is a major concern due to the high percentage of cases and mortality (LU et al., 2019).

1.7 Redox Metabolism

Malaria parasites are characterized by high adaptability to environmental conditions. One essential system for parasites' homeostasis is redox metabolism, which is crucial for redox balance and antioxidant defense and is also involved in drug action and resistance (Müller, 2015). The parasite surpasses oxidative stress problems with a competent antioxidant defense system composed of glutathione and thioredoxin-related proteins (Rahbari et al., 2017). Besides the fact that it is crucial for erythrocytic stage survival, glutathione is also involved in CQ resistance (Mohring et al., 2017). More recently, it has been associated with ACTs resistance (Siddiqui et al., 2017). The glutathione redox system of the parasite is composed of NADPH, as electron donor, and the enzymes glutathione reductase (GR), and reduced/oxidized glutathione (GSH/GSSG) (Kasozi et al., 2013). During the antioxidant defence, GSH is oxidised by glutathione S-transferase 1 (GST1). In balance, the parasite GR acts by recycling GSSG, with NADPH expense, maintaining the reduced cellular profile (Müller, 2015). The GSH/GSSG thiol-switch is a central redox regulator and is an indicator of cellular oxidative stress and redox status. This redox couple plays the main role in detoxification of ROS derived from antimalarial drugs, hemoglobin digestion, and the hosts' immune system (Kasozi et al., 2013; Mohring et al., 2017).



Figure 3. Redox balance in *P. falciparum*. Representation of GSH-GSSG switch in malaria parasite to maintain the redox homeostasis. The antioxidant defence oxidates GSH generating GSSG by GST1. The GR maintains the reduced cellular profile by recycling GSSG into GSH with NADPH expense. Adapted from (Müller, 2015).

1.8 Genetically encoded biosensors

There are many struggles related to conventional methods for measuring cellular oxidative state, including GSH and GSSG levels. These methods have several associated issues like the disruption of cell integrity, limitations in GSH levels detection, and impossibility to perform dynamic measures (Kasozi et al., 2013). Recently, genetically encoded sensors have been developed to overcome most of the technical limitations paving the way for unprecedented studies of cellular physiology (Mohring et al., 2017).

1.8.1 hGrx1-roGFP2

The genetically encoded redox sensor hGrx1-roGFP2 constituted with human glutaredoxin-1 (hGrx1) coupled to a redox-sensitive green fluorescent protein (roGFP2) was demonstrated to be a reliable tool to explore redox metabolism in living malaria parasites. The capacity of detection of this sensor reports to nanomolar and millimolar changes in GSSG and GSH concentrations (Mohring et al., 2016). The redox balance is measured by a ratio of two excitation wavelengths (405 nm and 488 nm): oxidative stress induction reacts with the disulfide bond of the biosensor, increasing fluorescent intensity of the 405 nm emission peak and decreasing the 488 nm peak (Kasozi et al., 2013).

Our workgroup was able to test this tool by inserting the redox biosensor in a pDC2 plasmid and integrating it in a Dd2^{attB} strain. In addition, the redox stage of the transfected parasites was studied by flow cytometer analysis.

Despite its effectiveness in redox changes, hGrx1-roGFP2 works as a cytosolic probe, so different variations of this genetically encoded biosensor would be helpful to study the redox status of other cellular organelles, mechanisms of drug evasion, and drug trafficking.

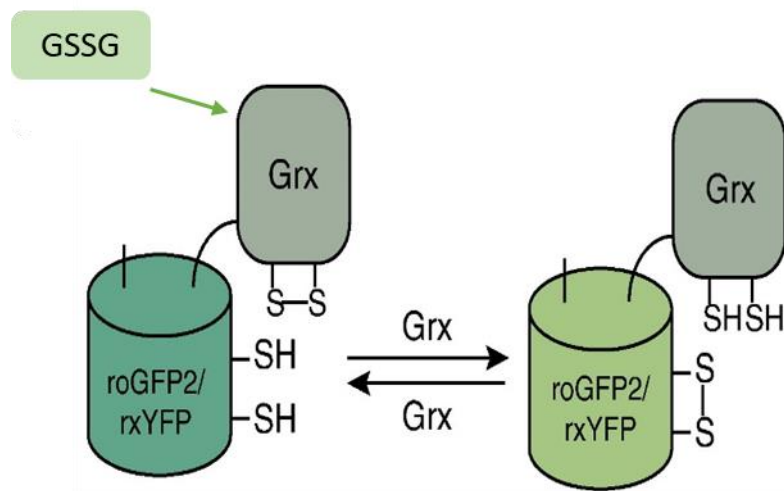


Figure 4. Schematic representation of the hGrx1-roGFP2 mode of action. The oxidized glutathione, GSSG, reacts with the human Grx of the sensor. This reaction promotes the switch of the cysteines, that are linked to the redox-sensitive GFP, modifying the fluorescence emission.

1.8.2 hGrx1-roGFP2-PEXEL

Red blood cells of the host are essential for the successful development of the infection. *P. falciparum* takes advantage of the host erythrocyte conditions and available components to grow and survive (Cowman et al., 2016b; De Koning-Ward et al., 2016). The export of different proteins from the parasite to the host RBC is essential for parasite survival and proliferation. The PTEX complex is responsible for the translocation of most of the proteins and is composed of a wide range of components that have specific functions and affinities to proteins (Loymunkong et al., 2019). Most of the exported proteins exhibit one of these components and have in common the *Plasmodium* exported element (PEXEL) (Nguyen et al., 2018), which is a motif that signals to export. When linked with PEXEL, the proteins bind to phosphatidylinositol-3-phosphate (PI3P) of the endoplasmatic reticulum (ER) membrane (Kalanon et al., 2016). In the ER, PEXEL is cleaved by the ER-resident aspartic protease Plasmepsin V (PMV), and the proteins pass through the membrane (Elsworth et al., 2014; Russo et al., 2010). This mechanism represents the most common way to translocate *Plasmodium* proteins into the host RBC (Russo et al., 2010).

Considering this, we aimed to create a genetically encoded biosensor linked to a PEXEL motif sequence, hGrx1-roGFP2-PEXEL. By integrating this biosensor into a parasite strain (3D7^{attB}), we expected to have a transgene parasite cell line in culture continuously expressing the biosensor and exporting it to the erythrocyte.

1.8.3 hGrx1-roGFP2-PEXEL-DD

The immunophilin protein-folding chaperone FKBP is called a destabilization domain (DD) (Minh & Hung, 2009), that when is fused to proteins, targets them for degradation in the proteasome (Filarsky et al., 2018). However, the presence of a cell-permeable small molecule ligand, Shield I, stabilizes the DD, thus preventing protein degradation (Usui et al., 2019). This system is functional in different cell types and organisms. Its efficacy in *P. falciparum* has been positively reported for studies of protein function, which is advantageous because it allows performing conditional regulation of genes or proteins (de Azevedo et al., 2012; Filarsky et al., 2018).

Therefore, we aimed to create a parasite line with a genetically encoded biosensor with conditional regulation. To do that, we wanted to construct a plasmid containing the genetically encoded biosensor coupled to the PEXEL sequence fused to the DD, hGrx1-roGFP2-PEXEL-DD. The expectation was to have a fluorescence biosensor that is only active in the presence of the stabilizing ligand.

1.8.4 hGrx1-roRFP

The use of green fluorescent protein (GFP) and its variants have been widely used as fluorescent biomarkers. Recently, a red-emitting variant of this protein was generated with an excitation around 550 nm and an emission peak at 585 nm (Toosi, 2014).

As stated before, the study of the redox balance is important in the knowledge of parasite biology, and genetically encoded biosensors are a strong tool for such studies (Shokhina et al., 2019). Furthermore, as these biosensors are encoded by genes which makes it possible to be integrated into the genome of the parasite, it also makes it possible to direct the biosensor to specific organelles of the cell and when using compatible fluorescences can be used simultaneously (Kasozi et al., 2013; Shokhina et al., 2019).

So, we aimed to create a genetically encoded biosensor with the red fluorescence emission. To do that, we pretended to substitute the roGFP2 of the hGrx1-roGFP2 with a roRFP biosensor. This sensor consists of the GFP variant with red emission (RFP) inside of the already successfully tested biosensor hGrx1-roGFP2. If it results, this tool would be helpful in parallel use with the green one, as it will make it possible to have real-time studies with two different emission fluorescences, red and green. The establishment of this new biosensor would correspond to a novel and efficient way to better understand *P. falciparum* biology.

1.9 Genetic engineering – Bxb1 integrase system

The haploid genome makes genetic manipulation of *P. falciparum* a challenge. Minor alterations in parasite DNA can lead to significant consequences such as death or development problems. The mycobacteriophage Bxb1 integrase (attB-attP) system presents an alternative approach for a more secure manipulation (Nkrumah et al., 2006) Since this system requires the use of genetically modified lines containing the attB site, such as the 3D7^{attB}, integrated at

the non-essential, in the blood stages, *cg6* locus (De Koning-Ward et al., 2015). The Bxb1 integrase rapidly expressed in the parasite's nucleus can efficiently catalyze the recombination between an attP-containing plasmid and an attB site integrated into the parasite genome. An attP-containing plasmid also encompassing a gene of interest can be used to insert a copy of this gene in the parasite genome (De Koning-Ward et al., 2015; Nkrumah et al., 2006). This technique has already been successfully employed in *P. falciparum* (Spalding et al., 2010).

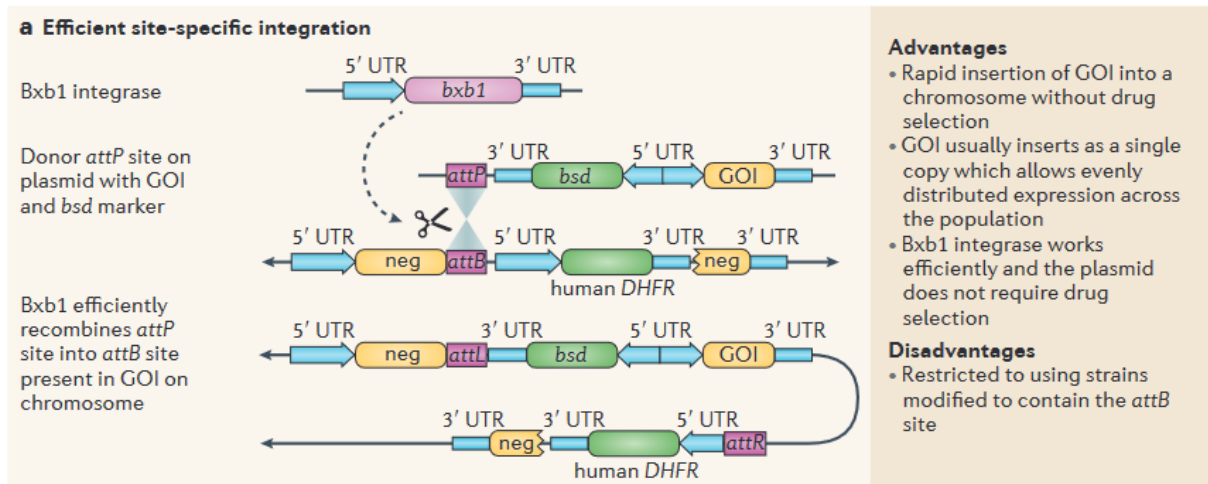


Figure 5. Plasmodium spp. genetic manipulation using the Bxb1 integrase system. The Bxb1 integrase system allows site-specific integration of interest plasmids into the Plasmodium spp. genome, by attB-attP sites recombination. (De Koning-Ward et al., 2015).

2. Aims

P. falciparum represents a global problem due to the increase in drug resistance strategies (Blasco et al., 2017). Therefore, studies on parasite biology, parasite-host interactions, and mechanisms of drug action are urgently needed. More profound knowledge of the redox metabolism of the parasite represents a step forward in understanding parasite biology. One effective way to perform these studies is by using redox genetic encoded biosensors due to their sensitivity to oxidative status changes (Kasozi et al., 2013).

Taking this into account, this project aims to evaluate the impact of antimalarials in the erythrocyte host cells. Therefore, a recombinant strain of *P. falciparum* will be transfected, using the attB × attP integration method (Spalding et al., 2010), with a plasmid containing the hGrx1-roGFP2 biosensor coupled to a PEXEL sequence (De Koning-Ward et al., 2016). Also, this new biosensor will be coupled to a DD to have conditional regulation by addition of Shiel-I (Filarsky et al., 2018). Genomic integration of these plasmids allows maintaining the plasmid stable on continuous culture without selective drugs exposure. The goal of having these tools integrated into a *P. falciparum* strain and being exported to the host RBCs is to reveal the impact of the drugs in host-parasite interaction.

The construction of a new hGrx1-roGFP2 biosensor with red fluorescence emission, the hGrx1-roRFP, is also expected. This sensor consists of the GFP variant with red emission (RFP) inside of the already successfully tested biosensor hGrx1-roGFP2 (Toosi, 2014). A positive result in this construction will enable the parallel usage of two different fluorescent biosensors and perform real-time studies with two different emission fluorescence, red and green.

The impact of these biosensors can be huge, as these are encoded by genes that make it possible to be integrated into the parasite's genome. It also makes it possible to direct the biosensor to specific cell organelles and, when using compatible fluorescence, can be used simultaneously.

Summing up, this project aims to achieve the following objectives:

- Construction of three genetically encoded biosensors derived from hGrx1-roGFP2 - hGrx1-roGFP2-PEXEL, hGrx1-roGFP2-PEXEL, and hGrx1-roRFP.
- Validation of the generated biosensors activity.
- Study the oxidative stress responses of the parasite to oxidation and reduction induction by fluorescence emission analyses.

3. Materials and Methods

3.1 Plasmids construction

Plasmid sequence of pDC2 was provided by Marcus Lee, Sanger Institute; pINT was obtained from Addgene, and pGDV1 was kindly provided by Till Voss Swiss Tropical Institute, University of Basel.

The cloning strategies were designed *in silico* using the software Ape (Sun Microsystems, University of California, USA).

3.1.1 pJET_PEXEL construction

The PEXEL fragment was first inserted in the pJET Cloning Vector 1.2/blunt (CloneJET PCR Cloning Kit, Thermo Fisher Scientific) following the producer's indications for the sticky end product. This reaction results in the ligation of the insert with the pJET. The transformation was performed using NZY5 α [®] competent cells (NZYTech) applying the heat shock transformation method. More specifically, the *E. coli* competent cells were thawed on ice for 15 minutes, then the ligation product from CloneJET PCR Cloning Kit was added in 10% of *E. coli* cells volume. The mixture was left on ice for 20 minutes. After the incubation, cells were heat-shocked at 42° for 40 seconds on a thermoblock and then placed on ice for 2 minutes. The recovery of the cells was performed by adding 300 μ L of Super Optimal broth with Catabolite repression (SOC) medium [20 g/L bacto-tryptone, 5 g/L bacto yeast extract, 10 mM NaCl, 2.5 mM KCl, 0.1M MgCl₂, 10 mM MgSO₄ and 20 mM glucose], and were then placed at 37° with shaking, at 200 rotation per minute (rpm), 1 hour. The cells were plated into lysogeny broth (LB) [10 g/L bacto-tryptone, 5 g/L yeast extract, and 10 g/L NaCl] agar plates supplemented with ampicillin antibiotic (100 μ g/ml) and incubated overnight at 37°C. Ampicillin was chosen due to a resistance cassette for this drug in the plasmid of interest.

Two colonies were selected and expanded the day after into 5 mL of LB liquid medium supplemented with ampicillin (100 μ g/ml), at 37°C, with shaking, overnight. First, Plasmid DNA isolation was performed using the Zippy[™] Plasmid Miniprep Kit (Zymo Research). Then, concentration and purity of the plasmid were measured using NanoDrop[™] 1000 spectrophotometer (Thermo Scientific). At last, to check if the plasmids extracted were

correct, the BglII restriction enzyme (New England Biolabs®, Inc) was used following manufacturer recommendations.

3.1.2 pDC2_hGrx1_roGFP_PEXEL construction

To create the pDC2_roGFP_PEXEL, two plasmids were used, pDC2_roGFP and pJET_PEXEL. First, PEXEL insert was amplified from pJET_PEXEL by a polymerase chain reaction (PCR). This PCR was made using 0.5µg of DNA template, 0.5µM of each primer, P1, and P2 (Table 1), 255µL of Supreme NZYtaq II 2× Green Master Mix (NZYTech, Lda) and nuclease-free water to a final volume of 50µL. The first step was DNA template denaturation, 5 minutes at 95°. Then a 35 cycles program was initiated following polymerase manufacturer indications – 94° for 30 sec, 63° for 30 sec, and 72° for 15 sec. At last, it was 5 min at 72° for final extension and left at 4° until tubes collection. In parallel, pDC2_roGFP was restricted with AvrII and NheI (New England Biolabs®, Inc), following manufacturer protocol.

The products from the PCR and restriction reactions were analyzed by electrophoresis in an agarose gel (1%), using a molecular weight marker (GeneRuler 1kb DNA Ladder, Thermo Fisher Scientific). The bands of interest, 299bp in pJET_PEXEL and 7547 in pDC2_roGFP, were cut from the gel and cleaned using NZYGelpure (NZYTech, Lda).

The ligation of the two products was obtained by NZYEasy Cloning & Expression kits (NZYTech, Lda), replacing the vector from the kit with the pDC2_roGFP product. Different times for the first step of the reaction were tested – 5, 15, and 30 minutes – to optimize it. Then, the ligation product was transformed by heat shock method, and DNA was isolated with Zypzy™ Plasmid Miniprep Kit (Zymo Research) as previously described (2.2.1.1). Finally, the plasmids isolated from colonies were digested with XmnI (New England Biolabs®, Inc), and the ones with the correct pattern were sent for sequencing.

Table 1. Primer sequences for plasmid construction.

Name	Primer Sequence (5'→3')	Tm
P1	ATAGAAATATATCACCTAGGATGAAAAGTTTTAAGAACAA	59°C
P2	CCCTTTGAGAACTCGCTAGCCTGTGGAGCTTGATGGTTTA	70°C
P5	AGAACCTATTCTTGCAAATACCGTTCTAGTATGGGAGTG	66°C
P6	AATATATTATATAACTCGAGTTAGCATAACTTAAAGGGCT	68°C

3.1.3 pDC2_hGrx1_roGFP_PEXEL_DD construction

Two plasmids were manipulated to construct pDC2_roGFP_PEXEL_DD, pDC2_roGFP_PEXEL, and pGDV1. A PCR was performed in pGDV1 to amplify the DD sequence, the reaction was like the one described before (2.2.2) using primers P5 and P6 (Table 1) and an annealing temperature of 59°. The pDC2_roGFP_PEXEL was digested with XhoI (New England Biolabs®, Inc). Then, to avoid re-ligation, it was incubated with Quick CIP (New England Biolabs®, Inc) for dephosphorylation of DNA ends. The primers used in the PCR were designed to amplify DD from pGDV1 and have specific overhangs with homology to the overhangs generated in pDC2_roGFP_PEXEL after digestion.

NZYEasy Cloning & Expression kits (NZYTech, Lda) were used for products ligation. The ligation was transformed by heat shock, and the plasmid was extracted with Zyppy™ Plasmid Miniprep Kit (Zymo Research) (methods described at 2.2.2). DNA was digested with AgeI and EcoRV (New England Biolabs®, Inc) to genotype and then sent to sequencing.

3.1.4 pDC2_roRFP construction

To create pDc2_roRFP, pJET_roRFP was first constructed with RFP insert and pJET Cloning Vector 1.2/blunt (CloneJET PCR Cloning Kit, Thermo Fisher Scientific) the same way as pJET_PEXEL, described on 2.2.1. The roRFP gene was designed and then synthesized by IDT™.

The pDC2_roRFP plasmid was built by manipulating two plasmids, pDC2_roGFP, and pJET_roRFP. First, the pDC2_roGFP was digested with AvrII and XhoI (New England Biolabs®, Inc). At the same time, a PCR of pJET_roRFP was made to amplify the roRFP gene, as described at 2.1.2, with P15 forward primer and P16 reverse primer (Table 1), at an annealing

temperature of 50°. After electrophoresis in agarose gel (1%), bands were cutted-off from the gel, 6386bp from pDC2_roGFP and 1170bp from pJET_roRFP, and purified with NZYGelpure (NZYTech, Lda). Then, the ligation of the vector and the insert was made with T4 DNA Ligase (New England Biolabs®, Inc), following the suggested protocol. Finally, the product was transformed by the heat shock method, as mentioned before.

After expansion for miniprep and extraction with Zyppy™ Plasmid Miniprep Kit (Zymo Research), DNA was digested with HindIII (New England Biolabs®, Inc) and then sent for sequencing.

3.1.5 Plasmids preparation for transfection

The plasmids that were correct after sequencing were prepared to be transfected into *P. falciparum* cultures. For that, *E. coli* containing the parasite were expanded in 300µL of LB liquid medium, supplemented with ampicillin (100 µg/mL), at 37°C, with shacking at 200 rpm, overnight. Then, the plasmids were isolated using ZymoPURE™ II Plasmid Maxiprep Kit (Zymo Research) to extract high concentrations of plasmids. Next, the NanoDrop™ 1000 spectrophotometer (Thermo Scientific) measured concentration and purity. Samples were accepted when purity ratios were above 1.9 for 260/280 and 2 for 230/260.

3.2 *P. falciparum* transgene cell lines

3.2.1 *P.falciparum* culture

Parasites in the asexual stage were cultured with human RBCs in malaria culture medium (MCM) – [RPMI 1640 (Gibco) with 2 mM L-glutamine, 200 µM hypoxanthine, 0.25 µg/mL gentamycin, 25 mM HEPES, 0.2% NaHCO₃, and 0.25% Albumax II (Life Technologies)] under a controlled atmosphere of 5% O₂/5% CO₂/90% N₂ maintained in t25 culture flasks. Cultures were maintained at 4% hematocrit in 5 mL of MCM. Medium changes were performed daily with monitoring of cultures wellbeing.

3.2.2 *P. falciparum* growth analysis

P. falciparum cultures parasitemia was regularly counted by microscopy or flow cytometry. For the microscopic analysis, a blood smear was prepared, fixed with methanol 100%, and colored with 10% Giemsa's Azur eosin methylene blue solution (Merck) for 20 minutes. Parasitaemia was calculated by counting the number of parasitized erythrocytes per total of erythrocytes counted.

For the flow cytometry analysis, 10 μ L of *P.falciparum* culture were incubated with 40 μ L of staining solution [2X SYBR Green (Applied Biosystems) and 1.6 μ M mitotracker deep red (Applied Biosystems)] for 30 minutes at 37°C. After the incubation, 300 μ L of PBS was added, and the cells were analyzed on an LSRII flow cytometer (BD Biosciences. SYBR Green stains DNA (parasitized cells) and mitotracker stains based on mitochondrial membrane potential (alive parasites). Data were analyzed using FlowJo software (TreeStar). Gate was done on the SYBR Green and mitotracker positive cells giving the parasitemia present against the total number of cells.

3.2.3 *P. falciparum* transfection

The transfection process was performed by electroporating *P. falciparum* parasites into unparasitized erythrocytes as follows: first, the erythrocytes were washed with 5 mL of MCM and centrifuged to collect the erythrocytes, at 1500 xg for 5 minutes. Another wash step was performed with cytomix [10 mM/L K₂HPO₄/KH₂PO₄, 120 mM/L KCl, 0.15 mM/L CaCl₂, 5 mM/L MgCl₂, 25 mM/L HEPES, 2 mM/L EGTA, adjusted with 10 M/L KOH to pH 7.6]. A mixture was prepared with 50 μ g of each plasmid and cytomix to a final volume of 200 μ L and 300 μ L of the washed erythrocytes. The mixture was transferred to Pulser[®]/MicroPulser[™] Electroporation Cuvettes, 0.2 cm gap (BioRad), and the electroporation was performed at 0.31 kV with a capacitance of 950 μ F on the Gene Pulser Xcell[™] (BioRad) electroporator. After electroporation, two washes were made with 5 mL of MCM. The transfected RBCs were then inoculated with *P. falciparum* parasite erythrocytes at trophozoite stage with a 5% parasitemia in 5 mL of MCM.

To create the 3D7_PEXEL line, two plasmids (the pINT and the pDC2_roGFP_PEXEL) were co-transfected into the 3D7^{attB} strain.

To create the 3D7_PEXEL_DD line, two plasmids were co-transfected the pINT and the pDC2_roGFP_PEXEL_DD into the 3D7^{attB} strain.

To create the Hb3_roRFP line, the pDC2_roRFP plasmid was transfected into the Hb3 strain.

3.2.4 Selection of parasites

The transfected cultures were left to grow until they reached a parasitemia of ~4%. The 3D7_PEXEL and 3D7_PEXEL_DD cultures were double selected with 2.5 µg/mL blasticidin S HCl (BSD) (Sigma-Aldrich) that selects for pDC2_PEXEL and pDC2_PEXEL_DD and G418 that sets for integration (pINT). The G418 was added daily to the culture for 3 or 4 days, and BSD was added until no viable parasites were observed on microscope. Since the plasmid is episomal and not integrated, the Hb3_roRFP was selected with continuous addition of BSD.

3.2.5 Genotyping

After the selection process, when parasites reappeared, the cultures were genotyped to evaluate the success of the transfections. To do that, gDNA of each culture was extracted using the NZY Blood gDNA Isolation kit (NZYTech), following manufacturer recommendations.

A set of three PCRs were performed to genotype 3D7_PEXEL and 3D7_PEXEL_DD cultures (Table 2). These reactions allowed us to check if the plasmid was integrated into the parasites' genome.

Table 2. Primers' sequence and PCR program for 3D7_PEXEL and 3D7_PEXEL_DD genotyping.

Line	Primers		PCR Programme	Meaning	
PEXEL	P19	GATAGCGATTTTTTTTACTGTCTG	3'1	95°C – 5'; 35 cycles: 94	Positive ->
	P20	AAATGTATAAAAAGATGAACATGGTTTC	3'2	°C – 30'', 48°C – 30'', 72°C – 15''; 72 °C – 10'	Integrated
or	P21	GATGCGCAATTAACCCTCACTAAAGGG	5'1	95°C – 5'; 35 cycles: 94	Positive ->
PEXEL _DD	P22	GCACAGATGCGTAAGGAGAAAATA 5'2		°C – 30'', 56°C – 30'', 72°C – 15''; 72 °C – 10'	Integrated
	P21	GATGCGCAATTAACCCTCACTAAAGGG	5'1	95°C – 5'; 35 cycles: 94	Positive ->
	P20	AAATGTATAAAAAGATGAACATGGTTTC	3'2	°C – 30'', 52°C – 30'', 72°C – 15''; 72 °C – 10'	unintegrated

3.3 Phenotyping

3.3.1 3D7_PEXEL_DD fluorescence

The 3D7_PEXEL_DD line was observed with fluorescence microscopy to check for the biosensor fluorescence. A microscope slide was prepared with a drop of blood from the culture protected with a glass coverslip. The parasites were observed in an Olympus Widefield Upright Microscope BX61, under a 100x objective with green excitation (FITC). The culture was also analyzed using the flow cytometer. For that, a mixture of 20 µL of culture and 300 µL of PBS was prepared and evaluated in the LSRII flow cytometer (BD Biosciences) with 488nm excitation (FITC). A negative control (3D7^{attB}) was also added to ensure fluorescence positivity.

3.3.2 Shield assay on 3D7_PEXEL_DD

To promote the exit of the biosensor through the RBC by DD stabilization, Shield-I (Takara Bio Inc.®), a stabilization ligand, was added to the culture at a concentration of 0.31 µM during a complete erythrocyte cycle of the parasite (Filarsky et al., 2018). The culture was then observed with fluorescence microscopy and flow cytometry, and samples preparation and protocols were made as described before (2.3.1).

3.3.3 Confocal microscopy of Hb3_roRFP

The fluorescent activity of Hb3_roRFP was firstly checked with confocal microscopy. The samples preparation was prepared equally to the ones for fluorescence microscopy. The culture was observed in the Olympus LPS Confocal FV1000. Two lasers were used to excite parasites 488 nm (FITC) and 559 nm (Yellow laser). A manipulated cell line previously constructed, Hb3_roGP, was used as a control since this one only emits on the green spectrum. By contrast, Hb3_roRFP was expected to have both emissions, green and red.

3.3.4 Test of genetically encoded redox biosensor activity

After checking fluorescence on the confocal microscope, Hb3_roRFP was tested on the LSRII flow cytometer (BD Biosciences) to evaluate the redox biosensor activity. In this assay, Hb3_roGFP was used as a control and compared with the new transgene culture. Both cultures were maintained growing until they reached a 4% parasitemia. Then, a mixture for each culture was prepared, using 20 μ L of culture in 300 μ L of PBS. The cytometer protocol consisted of analyzing each sample in the flow cytometer under 2 conditions – baseline and oxidation induction with hydrogen peroxide (H_2O_2) 1mM or reduction induction with dithiothreitol (DTT) 0.5 mM. These conditions were observed during equal intervals of time, 1 minute for every one of them. First, the mixture was passed alone to get the redox baseline status. Then, DTT or H_2O_2 were added and analyzed for one more minute. The excitation was made by a 488 nm blue laser with acquisition in three channels – AmCyan, FITC, and PerCP-Cy5-5. Data were analyzed using FlowJo software (TreeStar, Oregon, USA).

3.3.5 Statistical Analysis

Statistical analysis was performed using the GraphPad Prism 7 software (California, USA). Results were presented as means \pm standard error of the mean (SEM). Comparisons between different conditions were performed using two-way ANOVA. Differences were considered significant in the statistical analysis when $p < 0,05$. At least three biological replicates were performed for each assay.

4. Results and Discussion

Malaria remains one of the major causes of illness and death worldwide, especially in tropical regions and in children. *P. falciparum* is the most virulent *Plasmodium spp.*, being responsible for most deaths and severe cases of the disease. This is related to its ability to evade the immune system by clearance of cytoadherence and obstructing perfusion (Cowman et al., 2016a). These facts make this species of particular interest, and therefore it's the focus of this dissertation.

The usage of ACTs as a first-line treatment has slowed the rate of malaria spread and associated deaths in the last years. However, the capacity of the parasite to overcome the drug effectiveness and generate mechanisms of drug resistance has already a negative impact on the reduction of malaria incidence. Furthermore, some of these mechanisms have been associated with the redox metabolism of the parasite, which is also crucial for parasites' survival and replication (Müller, 2015).

4.1 PEXEL and PEXEL_DD

4.1.1 Plasmids pDC2_hGrx1_roGFP_PEXEL and pDC2_hGrx1_roGFP_PEXEL_DD

Previous work in the redox metabolism of *P. falciparum* study served as the base for projecting new forms to better understand this system. Using an already in vivo tested genetically encoded biosensor, we proposed to construct a new biosensor to be transported from the parasite through the erythrocyte of the host. So, we designed the cloning strategy *in silico* (Figure 5. (A)). The products of the digestion of pDC2_hGrx1_roGFP with NheI and AvrII, and the product of the amplification of the PEXEL motif from pJET_PEXEL with primers P1 and P2, were ligated through recombinant homology between the overhangs left from enzyme digestion and the ones created from the primers used in the PCR. As the first time using this ligation method, 3 protocols were tested, with different time lengths, 5, 15, and 30 minutes. By genotyping the DNA isolated from positive colonies with digestion with XmnI (Figure 5. (A)), we attested the effectiveness of the plasmid construction pDC2_hGrx1_roGFP_PEXEL, in three replicates, being the 15 min protocol the most effective. This enzyme was chosen because it

cuts two times on the backbone plasmid and one time inside the PEXEL insert. We expected to use this plasmid to test redox balance inside the parasite and in the erythrocytic cytosol.

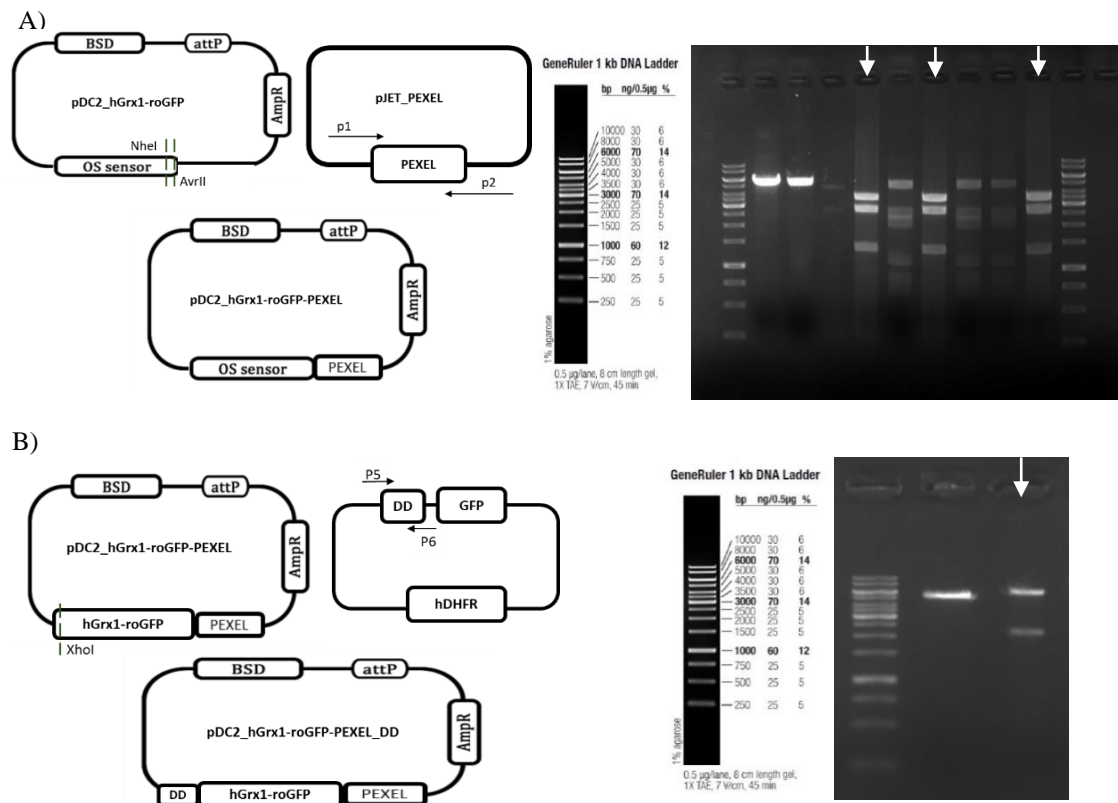


Figure 6. Strategy and plasmid construction for pDC2_hGrx1_roGFP_PEXEL and pDC2_hGrx1_roGFP_PEXEL_DD. A) In silico projection of pDC2_hGrx1-roGFP_PEXEL with pDC2_hGrx1-roGFP as backbone opened with NheI and AvrII restriction enzymes and amplification of the PEXEL insert from the pJET_PEXEL, previously made. The confirmation of the plasmid correctness was performed by digestion with XmnI, which cuts 2 times in the backbone plasmid and 1 in the insert, so 3 bands correspond to a correct plasmid. B) The pDC2_hGrx1-roGFP_PEXEL_DD development was dependent on the success of pDC2_hGrx1-roGFP_PEXEL. After confirmation of this one, a DD sequence was amplified with primers P5 and P6 from GDV1 plasmid, and pDC2_hGrx1-roGFP_PEXEL was opened with XhoI. To verify if the colonies were right, restriction digestion was made with AgeI that cuts in the insert and EcoRV that cuts in the backbone.

Besides being a novel tool for redox studies, there was no way to control the fluorescence emitted inside and out of the parasite. Therefore, the couple of a DD sequence would create a conditional regulation biosensor. So, we used the previously constructed plasmid pDC2_hGrx1-roGFP_PEXEL cut with XhoI as backbone and pGDV1 for DD amplification with P5 and P6 (Figure 5. (B)). Due to the efficacy of the homology method, we repeated it for this construction, but only for the 15 min protocol. The colonies check was

made by Agel, which cuts on the DD, and EcoRV, which cuts on the backbone, restriction, and we had a positive result in one isolated colony (Figure 5. (B)).

Overall, the projections made in silico were successfully achieved.

4.1.2 Transgene cell lines 3D7^{attB} roGFP_PEXEL and 3D7^{attB} roGFP_PEXEL_DD

The plasmids constructed, pDC2_hGrx1_roGFP_PEXEL and pDC2_hGrx1_roGFP_PEXEL_DD, were used to create two transgene parasite cultures. These two transfections aimed to generate parasites with a redox biosensor that is exported to the parasite, 3D7^{attB} roGFP_PEXEL and 3D7^{attB} roGFP_PEXEL_DD, this last one with the characteristic to be turned ON and OFF with the presence or absence of Shiel-I, respectively.

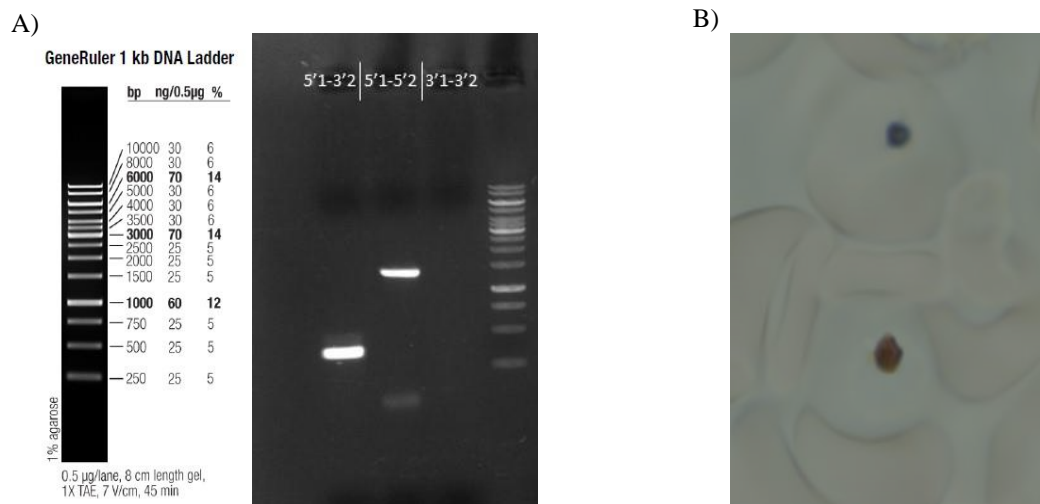


Figure 7. Genotyping and fluorescence excitation of parasites from 3D7^{attB} roGFP_PEXEL_DD. A) The transfected parasites were genotyped with specific primers after reappearance pos selection. The PCR showed the existence of nontransfected parasites by having band one the 5'1-3'2 primer mix. However, there was also a band that marks for plasmid integration on the attR, the correspondent to 5'1-5'2 pair. The amplification of the attL, 3'1-3'2 primers, was never accomplished, as is shown by the electrophoresis image. B) The transfected parasites were observed in fluorescence microscopy, in bright-field and green excitation (FITC). This observation was made after incubation of the culture with Shiel-I. The merge of the two acquired images for the same parasites showed no fluorescence emission.

To create the transgene cultures, each plasmid was co-transfected with pINT, a plasmid that promotes the expression of integrase 1, which promotes the reaction of the attB site of the parasite with the attP of the plasmid, abling the integration of the mutation into the parasite genome. These transfections were performed in an attB locus strain 3D7^{attB}.

The 3D7^{attB} roGFP_PEXEL was never accomplished. After three attempts, parasites didn't show up after BSD selection. This failure can be related to the construction protocol. The alterations made could lead to the loss of the plasmid efficacy.

However, the 3D7^{attB} roGFP_PEXEL_DD transfection had a different result. This line passed through selection and survived. We genotyped with primers for the plasmid integration, and we saw that should have occurred a problem in the integration reaction (Figure 6 (A)). The amplification with primers 5'1-3'2 marked the unintegrated parasites, and the PCRs with 5'1-5'2 and 3'1-3'2 for the integrated ones. The 3'1-3'2 was negative, in several repetitions, which indicated that the attR locus was not there, so there was no integration in this site (Figure 6 (A)). This integration failure could be due to the modifications performed in the backbone plasmid. The insertion of the DD sequence could have resulted in a plasmid without the capacity to integrate into the right site of the attB.

Nevertheless, as it had integrated into the left side, we proceeded to test the parasites' fluorescence. To do so, we added the Shield-I to the transfected culture and let it incubate for 48h, to a complete erythrocytic cycle. Then, we observed the parasites on the microscope in a green fluorescence channel (FITC), but no emission was detected (Figure 6 (B)).

As in the 3D7^{attB} roGFP_PEXEL case, these negative outcomes can be due to the genetic manipulation of the sensor, enabling its normal function.

4.2 roRFP genetically encoded biosensor

As an alternative to the failed results, a new strategy was designed to generate a genetically encoded biosensor with different specifications from the one available (hGrx1-roGFP2), a variant with red fluorescence emission.

4.2.1 pDC2_roRFP

A new redox biosensor was designed *in silico* and sent to synthesize. This insert was placed successfully in a pJET plasmid, pJET_roRFP. The confirmation of the colonies was made by digestion of DNA from colonies with XhoI, which cuts before and after the insertion site of the fragment and generates a band of the insert size, 1190 bp (Figure 7. left). This insert was then amplified with P15 and P16 and ligated by homology with pDC2_hGrx1_roGFP2 digested with AvrII and XhoI, which retrieved the roGFP2 sequence. Finally, the verification was made by digestion with HindIII, which cuts three times if the roRFP insert is in the plasmid (Figure 7. right).

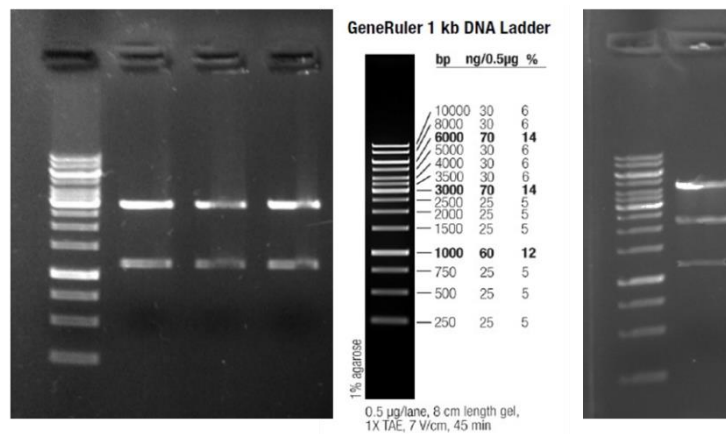


Figure 8. Genotyping of plasmids pJET_roRFP and pDC2_gGrx1_roRFP. The roRFP gene was designed *in silico*, and we bought the synthesized sequence. This was then inserted in a pJET plasmid. To confirm the plasmid DNA extracted from positive colonies was digested with XhoI. The three replicates of left electrophoresis gel were considered right due to the appearance of a band with the insert length, 1190 bp. The pDC2_hGrx1_roGFP was used as a backbone for the new biosensor. This plasmid was digested with AvrII and XhoI and fused with the biosensor amplified from pJET_roRFP with P15 and P16. The final plasmid, pDC2_hGrx1_roRFP, was confirmed by digestion of the isolated DNA with HindIII. The electrophoresis gel on the right shows three bands, consisting of the fusion of the two products.

4.2.2 Phenotyping of Hb3 roRFP transgene culture

The positive outcome from the plasmid construction took us to generate a transgene culture containing the red fluorescence biosensor. The pDC2_roRFP was transfected in a Hb3 WT culture and selected with BSD. The selection with this drug was because of a resistance

cassette for it in the plasmid. After parasites appearance, the culture was phenotyped by observation in a confocal microscope.

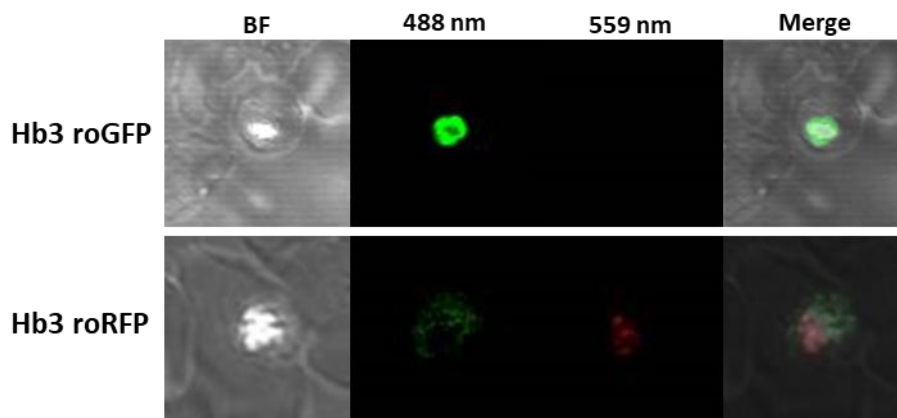


Figure 9. Confocal microscopy of Hb3 roGFP and roRFP lines. To phenotype the transfected parasites with the hGrx1-roRFP biosensor, the culture was observed under fluorescence excitation in a confocal microscope. Parasites from a Hb3 roGFP culture were used as a negative control for the red fluorescence. The two cultures showed fluorescence on the green channel, but only Hb3 roRFP emitted red fluorescence when excited with a 559 nm Yellow laser.

To validate the phenotype of the new transgene parasites, a comparison was made with a previously verified parasite line, the Hb3 roGFP, that has an effective green fluorescence biosensor. These controlling parasites are excited at 405 and 488 nm, only emitting on the green spectrum. On the other hand, the Hb3 roRFP line was expected to emit fluorescence at the green wavelength when excited with 488 nm and at the red range when excited with a 559 nm laser.

Under excitation with a 488 nm laser, both roGFR and roRFP emitted green fluorescence as expected. The actual confirmation of the new fluorescent parasites was when, under 559 nm excitation, only Hb3 roRFP emits red fluorescence, which was not observed at Hb3 roGFP (Figure 8).

These data have validated the fluorescence capacity of the parasites to emission in two different wavelengths with two different emission colors.

4.2.3 Hb3 roRFP biosensor activity

The validation of the fluorescence capacity of the parasites pushed us to the next phase, the confirmation of the biosensor activity. The Hb3 roGFP was again used as control as it was already validated.

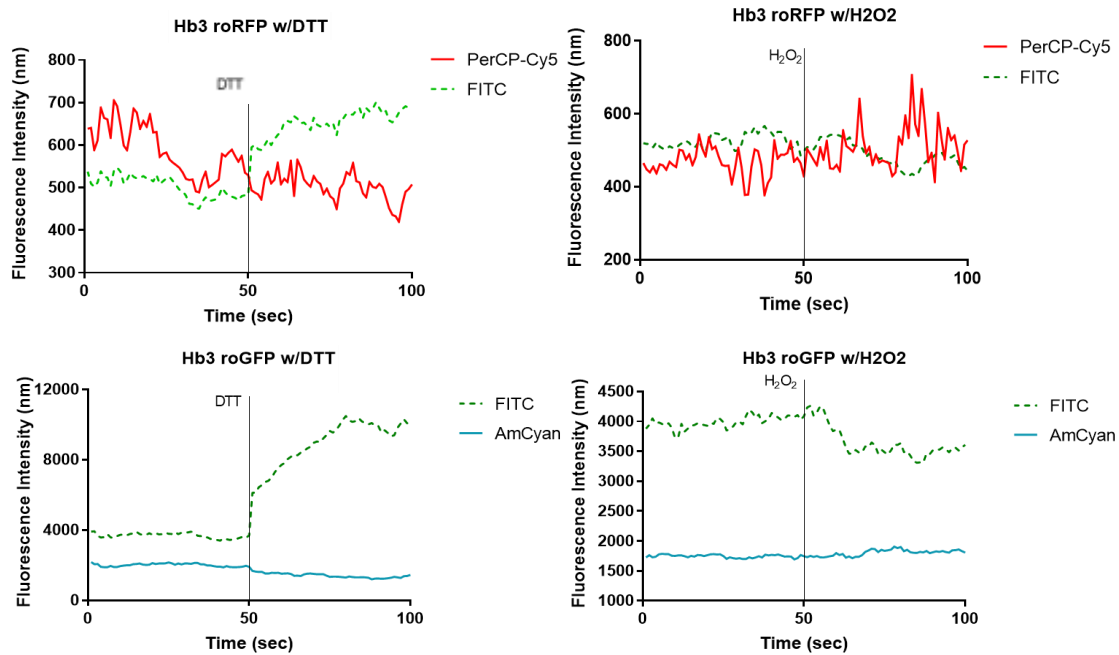


Figure 10. Validation of efficacy of the genetically encoded fluorescent biosensor in response to redox stimulus. The Hb3 roRFP and GFP lines were analyzed in a flow cytometer to check the fluorescence emission. The two strains of parasites have one similar channel of emission (FITC) and one that differs, PerCP-Cy5 for Hb3 roRFP and AmCyan for Hb3 roGFP. Therefore, the analyses were made with the corresponding wavelength channels. At the middle of the reading, DTT and H₂O₂ were added, one at a time to check for the sensibility of the sensor to redox alterations.

The biosensor action was analyzed in a real-time experiment. The two cultures with the biosensors, Hb3 roGFP, and roRFP, were analyzed in a flow cytometer.

The baseline of the oxidative status was first registered, followed by a redox stimulus induction. They were both stimulated with DTT and H₂O₂ to check the response of two contrary redox alterations, reduction, and oxidation, respectively.

This study allowed us to know that the biosensor worked in both cell lines. The behavior of the parasites' fluorescence to stimuli was similar with the wavelength in common, the 488 nm (FITC), going up with DTT, and lowering with H₂O₂ addition. However, the red

fluorescence emission had an opposite response to the drugs compared to the green one, decreasing with oxidation, DTT, and increasing with oxidation, H₂O₂ (Figure 8).

The variation of fluorescence intensity with induction of redox alterations and the different responses of wavelength emissions led us to analyze the ratio of the two wavelengths of emission. The ratio calculation gave us the biosensor dynamics, which was measured to the baseline, without drug add, and with drug stimulus for both drugs. The ratio of Hb3 roRFP was PerCP-Cy5/FITC, and for Hb3 roGFP, the ratio was FITC/AmCyan.

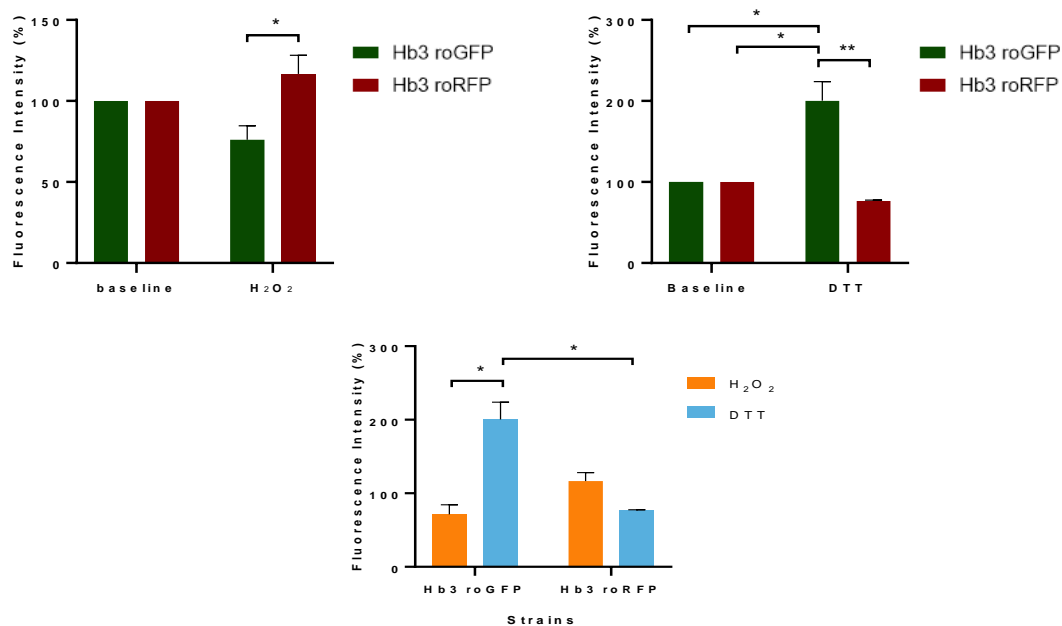


Figure 11. Comparison of Hb3 roRFP and Hb3 roGFP biosensors response to different oxidative statuses. The fluorescence intensity was calculated with the ratio PercP-Cy5/FITC for Hb3 roRFP and FITC/AmCyan for Hb3 roGFP. The response of both biosensors to redox alterations induced to DTT or H₂O₂ was measured and compared between the two cell lines, respectively (A) and (B). An analysis of the response of each parasite line to the different drugs was also made to see the effect of the redox status modification in the biosensor emission fluorescence (C).

The data were analyzed in GraphPad Prism 7, and two-way ANOVA tests were made to compare the different conditions. The baseline of each culture was normalized to 100%.

Statistically significant differences were detected between the two lines when responding to H₂O₂, but not between the baselines and the stimuli. Considering the DTT action, parasites had statistically significant differences in response to the drug induction, with

Hb3 roRFP having a notable reduction in fluorescence intensity and Hb3 roGFP an enormous increase. There were also significant differences between the baseline of Hb3 roGFP and the response to the stimulus (Figure 9).

The responses of each culture to DTT and H₂O₂ were also compared within. The responses of Hb3 roGFP to the two stimuli were statistically significantly different, with a considerable decrease with H₂O₂ addition and a raise in DTT response. The response of the different parasite lines to the same drug was again shown as significant (Figure 9).

These results together supported the capacity of the biosensor to recognize alterations in the oxidative status. Also, these show that they didn't only react differently to the stimuli compared one cell line to the other, as the same cell line has significant differences in response to the different drugs.

The results also sustained the importance of the redox metabolism, as it reacts to the induced changes in a matter of seconds. So it is secure to assume that this system is in constant action to maintain the parasite alive and healthy.

5. Conclusion

Malaria remains a major worldwide disease, besides all the efforts to control it. *P. falciparum* is the *Plasmodium spp.* most responsible for the malaria devastating numbers of infections and deaths, and therefore more knowledge in its biology is in constant need.

Antimalarial drug treatment is still the most effective way to control the disease. Although vaccines are now being seen as a new alternative in malaria control, it lacks knowledge about their influence on the field. Consequently, this puts high pressure on the available antimalarial drugs. These are among the most widely used drugs in tropical areas. The intensified usage of these drugs associated with incomplete patient treatment contributes to the emergence of *P. falciparum* resistance (Wicht et al., 2020).

The most rapid way to reduce disease proliferation is through the usage of ACTs. These antimalarials remain the most effective in limiting the parasite growth, being used as a first-line treatment. However, the surge of related resistance problems is now a problem (Ross & Fidock, 2019).

These together make it urgent to know more about the parasite biology and mechanisms of drug action and parasites' resistance.

Redox metabolism is crucial for parasite survival and proliferation. It is also a target for some drugs' mechanisms of action, and it has been associated with drug resistance mechanisms. So, redox metabolism shows up as an interesting candidate for deeper studies in parasites' metabolism.

The genetically encoded biosensors already described have been reported as an effective tool in redox metabolism exploration, allowing real-time studies *in vitro*.

We could not achieve a functional roGFP trafficked at the infected erythrocyte. Therefore, we opted to develop a novel sensor compatible with roGFP.

The developed hGrx1-roRFP was successfully achieved. Furthermore, the Hb3 roRFP oxidative stress experiments validated the sensor activity and drugs' influence on the parasite's redox homeostasis.

Overall, this dissertation project represented a step forward into the development of tools to increment the knowledge of the oxidative-stress mechanisms of the malaria parasite. By having a strain capable of reacting to redox stimuli, several future assays can be performed to deep into the parasite biology.

Bibliography

- Blasco, B., Leroy, Di., & Fidock, D. A. (2017). Antimalarial drug resistance: linking *Plasmodium falciparum* parasite biology to the clinic. *Nature Medicine*, *23*(8), 917–928.
<https://doi.org/10.1038/nm.4381>
- Combrinck, J. M., Mabothe, T. E., Ncokazi, K. K., Ambele, M. A., Taylor, D., Smith, P. J., Hoppe, H. C., & Egan, T. J. (2013). Insights into the Role of Heme in the Mechanism of Action of Antimalarials NIH Public Access \$watermark-text \$watermark-text \$watermark-text. *ACS Chem Biol*, *8*(1), 133–137.
<https://doi.org/10.1021/cb300454t>.Insights
- Cotter, C., Sturrock, H. J. W., Hsiang, M. S., Liu, J., Phillips, A. A., Hwang, J., Gueye, C. S., Fullman, N., Gosling, R. D., & Feachem, R. G. A. (2013). The changing epidemiology of malaria elimination: New strategies for new challenges. *The Lancet*, *382*(9895), 900–911. [https://doi.org/10.1016/S0140-6736\(13\)60310-4](https://doi.org/10.1016/S0140-6736(13)60310-4)
- Cowman, A. F., Healer, J., Marapana, D., & Marsh, K. (2016a). Malaria: Biology and Disease. *Cell*, *167*(3), 610–624. <https://doi.org/10.1016/j.cell.2016.07.055>
- Cowman, A. F., Healer, J., Marapana, D., & Marsh, K. (2016b). Malaria: Biology and Disease. *Cell*, *167*(3), 610–624. <https://doi.org/10.1016/j.cell.2016.07.055>
- de Azevedo, M. F., Gilson, P. R., Gabriel, H. B., Simões, R. F., Angrisano, F., Baum, J., Crabb, B. S., & Wunderlich, G. (2012). Systematic analysis of FKBP inducible degradation domain tagging strategies for the human malaria parasite *Plasmodium falciparum*. *PLoS ONE*, *7*(7). <https://doi.org/10.1371/journal.pone.0040981>
- De Koning-Ward, T. F., Dixon, M. W. A., Tilley, L., & Gilson, P. R. (2016). *Plasmodium* species: Master renovators of their host cells. *Nature Reviews Microbiology*, *14*(8), 494–507.
<https://doi.org/10.1038/nrmicro.2016.79>
- De Koning-Ward, T. F., Gilson, P. R., & Crabb, B. S. (2015). Advances in molecular genetic systems in malaria. *Nature Reviews Microbiology*, *13*(6), 373–387.
<https://doi.org/10.1038/nrmicro3450>
- Dondorp, A. M., Nosten, F., Yi, P., Das, D., Phyto, A. P., Tarning, J., Ph, D., Lwin, K. M., Ariey, F., Hanpithakpong, W., Lee, S. J., Ringwald, P., Silamut, K., Herdman, T., An, S. S., Yeung, S., Socheat, D., & White, N. J. (2009). Artemisinin Resistance in. *Drug Therapy*, *361*(5), 455–

467. <http://www.ncbi.nlm.nih.gov/pubmed/21543403>
- Douine, M., Lazrek, Y., Blanchet, D., Pelleau, S., Chanlin, R., Corlin, F., Hureau, L., Volney, B., Hiwat, H., Vreden, S., Djossou, F., Demar, M., Nacher, M., & Musset, L. (2018). Predictors of antimalarial self-medication in illegal gold miners in French Guiana: A pathway towards artemisinin resistance. *Journal of Antimicrobial Chemotherapy*, *73*(1), 231–239. <https://doi.org/10.1093/jac/dkx343>
- Eastman, R., & Fidock, D. (2009). ACTs: a vital tool in efforts to eliminate malaria. *Nature Reviews. Microbiology*, *7*(12), 864–874. <https://doi.org/10.1038/nrmicro2239>. Artemisinin-based
- Elsworth, B., Matthews, K., Nie, C. Q., Kalanon, M., Charnaud, S. C., Sanders, P. R., Chisholm, S. A., Counihan, N. A., Shaw, P. J., Pino, P., Chan, J. A., Azevedo, M. F., Rogerson, S. J., Beeson, J. G., Crabb, B. S., Gilson, P. R., & De Koning-Ward, T. F. (2014). PTEX is an essential nexus for protein export in malaria parasites. *Nature*, *511*(7511), 587–591. <https://doi.org/10.1038/nature13555>
- Ferreira, P. E., Culleton, R., Gil, J. P., & Meshnick, S. R. (2013). Artemisinin resistance in *Plasmodium falciparum*: what is it really? *Trends in Parasitology*, *29*(7), 318–320. <https://doi.org/10.1016/j.pt.2013.05.002>
- Filarsky, M., Fraschka, S. A., Niederwieser, I., Brancucci, N. M. B., Carrington, E., Carrió, E., Moes, S., Jenoe, P., Bártfai, R., & Voss, T. S. (2018). GDV1 induces sexual commitment of malaria parasites by antagonizing HP1-dependent gene silencing. *Science*, *359*(6381), 1259–1263. <https://doi.org/10.1126/science.aan6042>
- Josling, G. A., & Llinás, M. (2015). Sexual development in *Plasmodium* parasites: Knowing when it's time to commit. In *Nature Reviews Microbiology*. <https://doi.org/10.1038/nrmicro3519>
- Kalanon, M., Bargieri, D., Sturm, A., Matthews, K., Ghosh, S., Goodman, C. D., Thiberge, S., Mollard, V., Mcfadden, G. I., Ménard, R., & de Koning-Ward, T. F. (2016). The *Plasmodium* translocon of exported proteins component EXP2 is critical for establishing a patent malaria infection in mice. *Cellular Microbiology*, *18*(3), 399–412. <https://doi.org/10.1111/cmi.12520>
- Kano, S. (2010). Artemisinin-based combination therapies and their introduction in Japan. *Journal of Infection and Chemotherapy*, *16*(6), 375–382. <https://doi.org/10.1007/s10156-010-0077-1>

- Kasozi, D., Mohring, F., Rahlfs, S., Meyer, A. J., & Becker, K. (2013). Real-Time Imaging of the Intracellular Glutathione Redox Potential in the Malaria Parasite *Plasmodium falciparum*. *PLoS Pathogens*. <https://doi.org/10.1371/journal.ppat.1003782>
- Krishnan, K. M., & Williamson, K. C. (2018). The proteasome as a target to combat malaria: hits and misses. *Translational Research*, *198*, 40–47. <https://doi.org/10.1016/j.trsl.2018.04.007>
- Loymunkong, C., Sittikul, P., Songtawee, N., Wongpanya, R., & Boonyalai, N. (2019). Yield improvement and enzymatic dissection of *Plasmodium falciparum* plasmepsin V. *Molecular and Biochemical Parasitology*, *231*(December 2018), 111188. <https://doi.org/10.1016/j.molbiopara.2019.111188>
- LU, F., HE, X. L., Richard, C., & CAO, J. (2019). A brief history of artemisinin: Modes of action and mechanisms of resistance. *Chinese Journal of Natural Medicines*, *17*(5), 331–336. [https://doi.org/10.1016/S1875-5364\(19\)30038-X](https://doi.org/10.1016/S1875-5364(19)30038-X)
- Minh, H. Van, & Hung, N. (2009). Environmental Health Insights. *Environmental Health*, *8*, 63–70. <https://doi.org/10.4137/EHI.S8199>
- Mishra, M., Mishra, V. K., Kashaw, V., Iyer, A. K., & Kashaw, S. K. (2017). Comprehensive review on various strategies for antimalarial drug discovery. *European Journal of Medicinal Chemistry*, *125*, 1300–1320. <https://doi.org/10.1016/j.ejmech.2016.11.025>
- Mohring, F., Jortzik, E., & Becker, K. (2016). Comparison of methods probing the intracellular redox milieu in *Plasmodium falciparum*. *Molecular and Biochemical Parasitology*. <https://doi.org/10.1016/j.molbiopara.2015.11.002>
- Mohring, F., Rahbari, M., Zechmann, B., Rahlfs, S., Przyborski, J. M., Meyer, A. J., & Becker, K. (2017). Determination of glutathione redox potential and pH value in subcellular compartments of malaria parasites. *Free Radical Biology and Medicine*. <https://doi.org/10.1016/j.freeradbiomed.2017.01.001>
- Müller, S. (2015). Role and regulation of glutathione metabolism in *Plasmodium falciparum*. In *Molecules*. <https://doi.org/10.3390/molecules200610511>
- Nájera, J. A., González-Silva, M., & Alonso, P. L. (2011). Some lessons for the future from the global malaria eradication programme (1955-1969). *PLoS Medicine*, *8*(1). <https://doi.org/10.1371/journal.pmed.1000412>
- Nguyen, W., Hodder, A. N., de Lezongard, R. B., Czabotar, P. E., Jarman, K. E., O'Neill, M. T., Thompson, J. K., Jousset Sabroux, H., Cowman, A. F., Boddey, J. A., & Sleeb, B. E.

- (2018). Enhanced antimalarial activity of plasmepsin V inhibitors by modification of the P2 position of PEXEL peptidomimetics. *European Journal of Medicinal Chemistry*, *154*, 182–198. <https://doi.org/10.1016/j.ejmech.2018.05.022>
- Nkrumah, L. J., Muhle, R. A., Moura, P. A., Ghosh, P., Hatfull, G. F., Jacobs, W. R., & Fidock, D. A. (2006). Efficient site-specific integration in *Plasmodium falciparum* chromosomes mediated by mycobacteriophage Bxb1 integrase. *Nature Methods*, *3*(8), 615–621. <https://doi.org/10.1038/nmeth904>
- Pannu, A. K. (2019). Malaria today: advances in management and control. *Tropical Doctor*, *49*(3), 160–164. <https://doi.org/10.1177/0049475519846382>
- Plewes, K., Leopold, S. J., Kingston, H. W. F., & Dondorp, A. M. (2019). Malaria: What's New in the Management of Malaria? *Infectious Disease Clinics of North America*, *33*(1), 39–60. <https://doi.org/10.1016/j.idc.2018.10.002>
- Rahbari, M., Rahlfs, S., Jortzik, E., Bogeski, I., & Becker, K. (2017). H₂O₂ dynamics in the malaria parasite *Plasmodium falciparum*. *PLoS ONE*, *12*(4), 1–23. <https://doi.org/10.1371/journal>
- Ross, L. S., & Fidock, D. A. (2019). Elucidating Mechanisms of Drug-Resistant *Plasmodium falciparum*. *Cell Host and Microbe*, *26*(1), 35–47. <https://doi.org/10.1016/j.chom.2019.06.001>
- Russo, I., Babbitt, S., Muralidharan, V., Butler, T., Oksman, A., & Goldberg, D. E. (2010). Plasmepsin v licenses *Plasmodium* proteins for export into the host erythrocyte. *Nature*, *463*(7281), 632–636. <https://doi.org/10.1038/nature08726>
- Sato, S. (2021). *Plasmodium*—a brief introduction to the parasites causing human malaria and their basic biology. *Journal of Physiological Anthropology*, *40*(1), 1. <https://doi.org/10.1186/s40101-020-00251-9>
- Shokhina, A. G., Kostyuk, A. I., Ermakova, Y. G., Panova, A. S., Staroverov, D. B., Egorov, E. S., Baranov, M. S., van Belle, G. J., Katschinski, D. M., Belousov, V. V., & Bilan, D. S. (2019). Red fluorescent redox-sensitive biosensor Grx1-roCherry. *Redox Biology*, *21*(December 2018), 101071. <https://doi.org/10.1016/j.redox.2018.101071>
- Siddiqui, G., Srivastava, A., Russell, A. S., & Creek, D. J. (2017). Multi-omics based identification of specific biochemical changes associated with PfKelch13-mutant artemisinin-resistant *Plasmodium falciparum*. *Journal of Infectious Diseases*, *215*(9), 1435–1444. <https://doi.org/10.1093/infdis/jix156>

- Spalding, M. D., Allary, M., Gallagher, J. R., & Prigge, S. T. (2010). Validation of a modified method for Bxb1 mycobacteriophage integrase-mediated recombination in *Plasmodium falciparum* by localization of the H-protein of the glycine cleavage complex to the mitochondrion. *Molecular and Biochemical Parasitology*.
<https://doi.org/10.1016/j.molbiopara.2010.04.005>
- Sridaran, S., McClintock, S. K., Syphard, L. M., Herman, K. M., Barnwell, J. W., & Udhayakumar, V. (2010). Anti-folate drug resistance in Africa: Meta-analysis of reported dihydrofolate reductase (dhfr) and dihydropteroate synthase (dhps) mutant genotype frequencies in African *Plasmodium falciparum* parasite populations. *Malaria Journal*, 9(1), 1–22. <https://doi.org/10.1186/1475-2875-9-247>
- Talman, A. M., Clain, J., Duval, R., Ménard, R., & Ariey, F. (2019). Artemisinin Bioactivity and Resistance in Malaria Parasites. *Trends in Parasitology*, 35(12), 953–963.
<https://doi.org/10.1016/j.pt.2019.09.005>
- Toosi, K. (2014). 基因的改变 NIH Public Access. *Bone*, 23(1), 1–7.
<https://doi.org/10.1021/bi702130s>
- Usui, M., Prajapati, S. K., Ayanful-Torgby, R., Acquah, F. K., Cudjoe, E., Kakaney, C., Amponsah, J. A., Obboh, E. K., Reddy, D. K., Barbeau, M. C., Simons, L. M., Czesny, B., Raiciulescu, S., Olsen, C., Abuaku, B. K., Amoah, L. E., & Williamson, K. C. (2019). *Plasmodium falciparum* sexual differentiation in malaria patients is associated with host factors and GDV1-dependent genes. *Nature Communications*, 10(1), 1–15.
<https://doi.org/10.1038/s41467-019-10172-6>
- Weiss, D. J., Lucas, T. C. D., Nguyen, M., Nandi, A. K., Bisanzio, D., Battle, K. E., Cameron, E., Twohig, K. A., Pfeffer, D. A., Rozier, J. A., Gibson, H. S., Rao, P. C., Casey, D., Bertozzi-Villa, A., Collins, E. L., Dalrymple, U., Gray, N., Harris, J. R., Howes, R. E., ... Gething, P. W. (2019). Mapping the global prevalence, incidence, and mortality of *Plasmodium falciparum*, 2000–17: a spatial and temporal modelling study. *The Lancet*, 394(10195), 322–331. [https://doi.org/10.1016/S0140-6736\(19\)31097-9](https://doi.org/10.1016/S0140-6736(19)31097-9)
- Wellems, T. E., & Plowe, C. V. (n.d.). *Chloroquine-Resistant Malaria*. 770–776.
- White, N. J. (2013). Pharmacokinetic and pharmacodynamic considerations in antimalarial dose optimization. *Antimicrobial Agents and Chemotherapy*, 57(12), 5792–5807.
<https://doi.org/10.1128/AAC.00287-13>

- White, N. J., Pukrittayakamee, S., Hien, T. T., Faiz, M. A., Mokuolu, O. A., & Dondorp, A. M. (2014). Malaria. *The Lancet*, 383(9918), 723–735. [https://doi.org/10.1016/S0140-6736\(13\)60024-0](https://doi.org/10.1016/S0140-6736(13)60024-0)
- World Health Organization. (2020). WHO World Malaria Report 2020. In *Malaria report 2020*.
- Zekar, L., & Sharman, T. (2020). *Plasmodium falciparum* Malaria. In *STAT Pearls*.